Automatica 100 (2019) 403–406

Contents lists available at ScienceDirect

Automatica

journal homepage: www.elsevier.com/locate/automatica

Technical communique

Active wave suppression in the interior of a one-dimensional domain☆

Lea Sirota *, Anuradha M. Annaswamy

Department of Mechanical Engineering, Massachusetts Institute of Technology, Cambridge, MA, United States

ARTICLE INFO

Article history:
Received 13 March 2018
Received in revised form 8 August 2018
Accepted 4 November 2018
Available online 10 December 2018

Keywords:
Wave suppression
Uni-directional waves
Active interior absorber

ABSTRACT

We consider the problem of creating an absorber in the interior of a system that supports one-dimensional wave propagation, such as a waveguide, using active control. The control goal is suppression of wave propagation beyond a prescribed region of the waveguide, but without perturbing the propagation within that region. Unlike boundary control, achieving full absorption in the interior introduces a challenge of creating both a non-transmitting and a non-reflecting sink. We overcome this challenge by introducing a near uni-directional control wave which is accomplished by using two concentrated actuators. The residual back-action wave is minimized based on the available control energy. We employ this control wave in two algorithms, a feed-forward and a feedback one, which we denote by Interior Wave Suppression. We illustrate the theoretical results through numerical simulation of an acoustic waveguide example.

1. Introduction

Suppression of propagation and reflection of waves is a matter of interest in diverse fields of engineering. Examples include mechanical vibration suppression (Inman, 2017; Sumer & Bernstein, 2012), acoustic noise cancellation (Bies, Hansen, & Howard, 2017), swing oscillation damping in power grids (Chakrabortty, 2012; Lesieutre, Scholtz, & Verghese, 2002; Sirota & Annaswamy, 2017, 2018; Thorp, Seyler, & Phadke, 1998), and even cloaking, (Sanchis et al. 2013). In this work we consider one-dimensional wave propagation as commonly obtained in waveguides, which is a typical environment in a variety of important applications. The representative example in this work is an acoustic waveguide, (Beranek and Mellow 2012).

Our goal is to create an absorber for propagating waves at a prescribed location in the interior of the waveguide, in which the incoming waves will be completely absorbed, i.e. without any transmission and reflection from the absorber. While a full absorber is usually associated with boundaries and implemented e.g. via impedance matching, we attempt to replicate the concept in the domain's interior, without any physical boundaries present. We aim to implement this absorber by means of active control, using a minimal amount of concentrated actuation and measurement devices.

Active control algorithms for wave suppression are the topic of volumes of literature, ranging from methods that rely on spatial discretization of the medium, see e.g. Inman (2017), to methods targeting the exact continuum system, such as Guo, Shao, and Krstic (2017), Krstic, Guo, Balogh, and Smyshlyaev (2008) and Sirota and Halevi (2010, 2014, 2015a, 2015b). In the vast majority of the existing approaches, and in particular in those listed above, the control action takes place along the system boundaries, known as boundary control. The underlying physical reasoning is that a control wave generated at a boundary is restricted to propagate in the outward direction only and can be thus designed to suppress a source wave reflected from that boundary, yielding a partial or full wave suppression. However, the interior absorber problem cannot be tackled directly by the existing boundary control methods. As is well known for one-dimensional wave propagation, any concentrated input in the interior generates two waves, a progressive and a regressive one. Therefore, even if one of these control waves is designed to suppress source waves beyond the actuation point, an undesired control back action wave will occur.

In this work we develop a method of near uni-directional wave generation in the interior of the one-dimensional domain (mathematically, on an infinite line). The presented method is inspired by Sirota and Annaswamy (2017, 2018), in which a first attempt to generate such a wave for a ring domain was reported. Interior uni-directional wave generation of a different context and methodology was reported in the literature, including few examples (Fu, Lian, Liu, Gan, & Li, 2011; Maeda & Colonius, 2017; Rodríguez-Fortuño et al., 2013). We design two control algorithms, a feed-forward and a feedback one, which employ the uni-directional control wave to suppress the absorber's transmittance. We denote the approach behind the algorithms by the Interior Wave

☆ This work was supported by the National Science Foundation, United States through the EAGER Grant, award number 1745547. The material in this paper was not presented at any conference. This paper was recommended for publication in revised form by Associate Editor Henrik Sandberg, Hitay Ozbay under the direction of Editor André L. Tits, Miroslav Krstic.

* Corresponding author.
E-mail addresses: lbeilkin@mit.edu (L. Sirota), aanna@mit.edu (A.M. Annaswamy).

https://doi.org/10.1016/j.automatica.2018.11.030
0005-1098/

Suppression control. The suppression of the absorber's reflectance, i.e. control backwave minimization, is determined by a trade-off with available control energy. The analytic results are verified using numerical simulation of an acoustic waveguide.

2. Problem statement

We address the problem of creating an active wave absorber at a prescribed location x_0 in the interior of a one-dimensional waveguide, which is illustrated in Fig. 1. It is assumed that the system is of infinite spatial extension $-\infty < x < \infty$, which is also equivalent to a finite length waveguide with a matched boundary impedance. The waves to be absorbed are induced by a source term denoted by Ψ. The location of Ψ is defined as $x = 0$ and we focus on the system's response at $x > 0$ only. The available control inputs are denoted by f and h. The goal is designing a control strategy for f and h to suppress wave propagation at $x > x_0$ without altering the propagation at $x < x_0$. The location of the control inputs is x_0 for f and h, and $x_0 - \varepsilon$ for $-h$. The reasoning behind this particular arrangement, as well as the determination of the distance ε, is the subject of Section 3. It is assumed that the wave propagation in the waveguide can be described by the classical wave equation (Graff, 2012),

$$\begin{aligned} c^2 y_{xx}(x,t) = y_{tt}(x,t) + \tfrac{1}{\rho}\left[f(t)+h(t)\right]\delta(x-x_0) \\ - \tfrac{1}{\rho}h(t)\delta(x-x_0-\varepsilon) + \tfrac{1}{\rho}\Psi(t)\delta(x), \end{aligned} \tag{1}$$

where $t \geq 0$ is time, $\delta(\cdot)$ is the Delta function and $c = \sqrt{T/\rho}$ is the wave propagation velocity along the x axis. In the acoustic waveguide example, the parameters ρ and T are the respective mass density and bulk modulus of the fluid, whereas $y(x,t)$ may stand for its pressure, velocity or displacement. Applying Laplace transform to (1) with respect to time and keeping, for convenience, the original notations for the transformed variables, $y_{tt}(x,t)$ becomes $s^2 y(x;s)$, and (1) then becomes a second order ordinary differential equation in x. Considering the velocity $v(x;s) = sy(x;s)$ as the variable of interest, the total solution is given by $v(x;s) = v_\Psi(x;s) + v_c(x;s)$, which is a superposition of source term waves, denoted by v_Ψ, and control waves, denoted by v_c,

$$\begin{aligned} v_\Psi(x;s) &= \frac{e^{-\tau_x s}}{2\phi}\Psi(s) \\ v_c(x;s) &= \frac{e^{-|\tau_x-\tau_{x_0}|s}}{2\phi}\begin{cases} f(s)+\left(1-e^{-\tau_\varepsilon s}\right)h(s), & x \geq x_0, \\ f(s)+\left(1-e^{+\tau_\varepsilon s}\right)h(s), & x \leq x_0-\varepsilon. \end{cases} \end{aligned} \tag{2}$$

The control waves are given in (2) in two regions of interest: to the right of x_0, where suppression of transmission is required, and to the left of the leftmost control input $-h$, where suppression of reflection (in terms of control backwave) is required. The time constants $\tau_x = \frac{x}{c}$ and $\tau_\varepsilon = \frac{\varepsilon}{c}$ indicate the time required for a wave to travel the respective distance x and ε. $\phi = \frac{T}{c}$ is the characteristic impedance. The absolute value in (2) indicates the relative locations of the input at x_0 and the output at x. The transfer function from each concentrated input to the velocity v in (2) is a scaled pure delay, which indicates that the output is a pure shift of the input. The propagating wave does not undergo any shape distortion, as expected for the non-dispersive system (1).

3. Near uni-directional wave generation

In this section we derive the relation between the control inputs f and h to generate a control wave that will tend to be uni-directional. Such a control wave is required for creating a simultaneously non-transmitting and non-reflecting absorber for wave propagation in the interior of the waveguide, as depicted in Fig. 1. Defining the relation between f and h as

$$h(s) = C_h(s)f(s), \quad C_h(s) = \frac{1}{\tau_\varepsilon\,(s+\eta)}, \tag{3}$$

where $\eta > 0$ is a design parameter, the response to the control inputs f and h in (2) becomes

$$v_c(x;s) = \frac{e^{-|\tau_x-\tau_{x_0}|s}}{2\phi}\begin{cases} Q(s)f(s), & x \geq x_0, \\ \overline{Q}(s)f(s), & x \leq x_0-\varepsilon, \end{cases} \tag{4}$$

where

$$\begin{aligned} Q(s) &= 1+A(s), \quad A(s) = \left(1-e^{-\tau_\varepsilon s}\right)C_h(s), \\ \overline{Q}(s) &= 1+\overline{A}(s), \quad \overline{A}(s) = \left(1-e^{+\tau_\varepsilon s}\right)C_h(s). \end{aligned} \tag{5}$$

As ε (the distance between actuators) and η (the free design parameter) become smaller, we obtain the limits

$$\begin{aligned} &\lim_{\varepsilon,\eta\to 0} A(s) = 1, \quad \lim_{\varepsilon,\eta\to 0}\overline{A}(s) = -1, \\ &\lim_{\varepsilon,\eta\to 0} Q(s) = 2, \quad \lim_{\varepsilon,\eta\to 0}\overline{Q}(s) = 0. \end{aligned} \tag{6}$$

The limits of $A(s)$ and $\overline{A}(s)$ in (6) indicate that the physical meaning of the relation (3) is a simultaneous temporal integration and spatial differentiation of the response to f. When the limits in (6) are approached, the control wave generated at x_0 travels in the positive x direction only, as indicated by (4). In practice, however, the wave generation methodology in (3)– (6) has limitations. First, the limits in (6) cannot be fully approached, since the physical distance ε between two actuators cannot be rendered exactly zero. Second, the design parameter η must be kept positive for stability of $C_h(s)$ at the origin. The wave generated by f and h, related as in (3), is thus *near* uni-directional, whose amplitude is determined by $Q(s)$. The amplitude of the residual backwave is determined by $\overline{Q}(s)$. Since both the amplitude and the convergence rate of h increase when ε and η decrease, it constitutes the trade-off with the backwave amplitude, as discussed in Section 4.3.

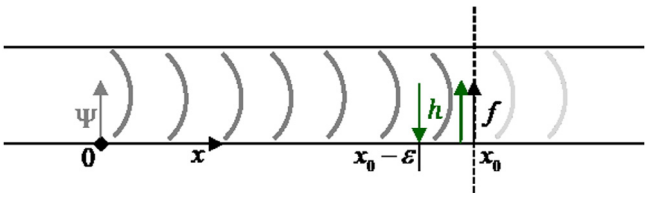

Fig. 1. Schematic diagram of a waveguide governed by the wave equation (1), for which we design an active absorber at an interior point x_0. Ψ is a source whose location is defined as $x = 0$. f and h are concentrated control inputs designed in Sections 3 and 4 to suppress transmission of Ψ waves to $x > x_0$, while simultaneously minimizing reflection to $x < x_0$.

4. Interior wave suppression control

In this section we derive the Interior Wave Suppression control algorithms to suppress transmission of source waves to $x > x_0$, while minimizing the control back action waves at $x < x_0$. The control actuation is carried out using the near uni-directional wave mechanism derived in Section 3, employing the net input f that results from relating inputs f and h via (3). We consider two different control setups (see Fig. 2). One is a feed-forward scheme, in which the source signal is measured in real time and is matched by f. The other is a feedback loop, in which the response at a point beyond x_0 is measured and minimized. For each setup we design a controller $C_f(s)$, which relates f to the measurement.

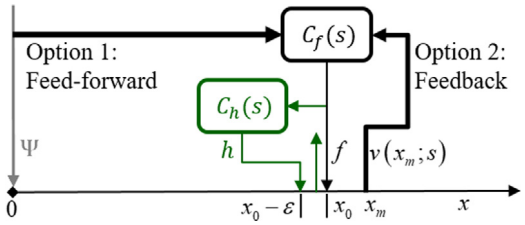

Fig. 2. Interior Wave Suppression control scheme illustrating two measurement options. Option 1 (Section 4.1) is a feed-forward of the source Ψ. Option 2 (Section 4.2) is a feedback of the velocity v at $x_m \geq x_0$. $C_h(s)$, (3), is a controller relating inputs h and f yielding a near uni-directional control wave. $C_f(s)$ is the controller designed for f to suppress propagation of Ψ waves at $x > x_0$.

4.1. Feed-forward control setup

In this section it is assumed that Ψ can be measured in real time, yielding the control law

$$f(s) = -C_f(s)\Psi(s). \tag{7}$$

To suppress propagation of Ψ waves beyond x_0, the control input needs to match the response to Ψ at x_0. The controller

$$C_f(s) = \frac{1}{Q(s)} e^{-\tau_{x_0} s} \tag{8}$$

brings the response in (2) to the form

$$v(x;s) = \frac{1}{2\phi} \begin{cases} 0, & x \geq x_0, \\ e^{-\tau_x s}\Psi(s) + BW, & x \leq x_0 - \varepsilon. \end{cases} \tag{9}$$

The net response at $x \geq x_0$ is zero, implying that an exact matching was obtained. BW is the backwave resulting from the control wave being near but not perfectly uni-directional. It is given by

$$BW = -\frac{1}{2\phi}\frac{\overline{Q}(s)}{Q(s)} e^{-(2\tau_{x_0}-\tau_x)s}\Psi(s). \tag{10}$$

The goal is minimizing the amplitude of BW, i.e. setting $\overline{Q}(s)$ to zero by an appropriate choice of ε and η in (3). The function $Q^{-1}(s)$ is proved to be stable in Section 4.4. For ease of implementation, $Q^{-1}(s)$ may be replaced by $\frac{1}{2}$ according to the limit in (6), compromising to some extent the exactness of the matching provided by (8). It should be noted, though, that since any realistic actuator has a finite bandwidth, there will be a certain mismatch of Ψ by f at $x \geq x_0$, which will tend to zero as faster f becomes available.

4.2. Feedback control setup

In this section we assume that the only measurable quantity is the response v available at $x_m \geq x_0$. The control law is then given by

$$f(s) = -C_f(s)v(x_m;s). \tag{11}$$

Assuming for brevity $x_m = x_0$, we design the feedback controller as

$$C_f(s) = \frac{2\phi}{Q(s)} C_0(s), \tag{12}$$

where $C_0(s)$ is a stabilizing sub-controller. The closed loop response then becomes

$$v(x;s) = \frac{1}{2\phi} \begin{cases} \dfrac{1}{1+C_0(s)} e^{-\tau_x s}\Psi(s), & x \geq x_0, \\ e^{-\tau_x s}\Psi(s) + \dfrac{C_0(s)}{1+C_0(s)} BW, & x \leq x_0 - \varepsilon, \end{cases} \tag{13}$$

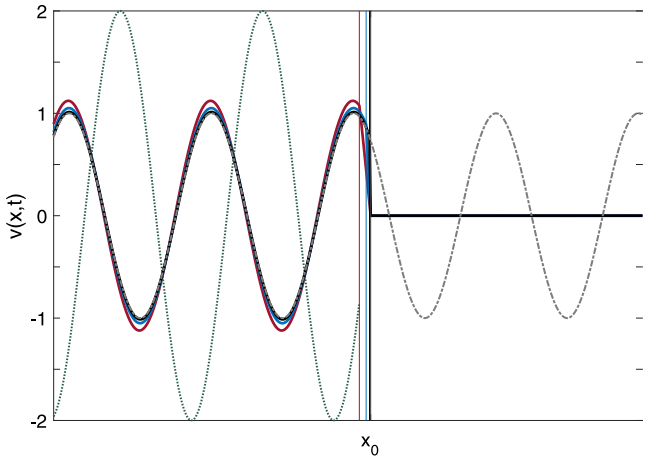

Fig. 3. Simulation of the active interior absorber in an acoustic waveguide example. The response to Ψ at $x = 0$ is depicted for the entire axis $x \geq 0$ at a fixed time instant. Grey: wave propagation with the absorber turned off. Red, blue, black: total wave propagation with the absorber turned on at x_0, created by control action at x_0 and $x_0 - \epsilon$ (vertical lines) according to (8) and (7), for $\epsilon = 0.05$ m (red), $\epsilon = 0.02$ m (blue) and $\epsilon = 0.005$ m (black), with $\eta = 500\epsilon$. Transmitted wave amplitude at $x > x_0$ is zero irrespective of ϵ. Reflected wave (backwave (10)) amplitude at $x < x_0$ decreases with ϵ. Dotted-green: the total wave at $x < x_0$ if only one control input was operating at x_0. (For interpretation of the references to colour in this figure legend, the reader is referred to the web version of this article.)

where the backwave BW is given in (10). The design of the sub-controller $C_0(s)$ depends on the frequency ω_0 of the source signal. For steady state suppression the poles of $C_0(s)$ need to resonate at ω_0, while suppression of the transients is also desired. As follows from (11)– (13), both the backwave BW and the control input h are proportional to $C_0(s)/(1 + C_0(s))$, implying that the trade-off between their amplitudes holds in the feedback setup as well.

4.3. Simulation and discussion

We demonstrate the effectiveness of the Interior Wave Suppression control approach through an example from acoustics. The waveguide in Fig. 1 is then a tube filled with air (speed of sound $c = 340$ m/s), with a circular cross-section sufficiently smaller than the wavelength to enable propagation according to (1), Beranek and Mellow (2012). The source, as well as the control inputs, are assumed to be generated by loudspeakers. A typical acoustic working frequency of $f_0 \approx 540$ Hz (wavelength $\lambda \approx 0.6$ m) and amplitude 1 was selected for the source Ψ. Fig. 3 depicts the wave propagation in the waveguide at a fixed time instant. The propagation when the absorber is turned off (grey) is compared to that when the absorber, generated according to the feed-forward control algorithm (Section 4.1), is turned on for $\varepsilon = 0.05$ m (red), $\varepsilon = 0.02$ m (blue) and $\varepsilon = 0.005$ m (black). The transmitted wave amplitude at $x > x_0$ is zero irrespective of ε. The reflected wave (backwave (10)) amplitude at $x < x_0$ decreases with ε. For $\varepsilon = 0.005$ m the total wave (black) is almost indistinguishable from the source wave (grey). The total wave at $x < x_0$ for only one control input operating at x_0 (dotted green), is depicted for comparison, yielding an amplitude twice than the source.

In Fig. 4 we tried to determine the efficiency of the proposed near uni-directional mechanism, i.e. how much control effort is required to achieve a particular reduction in the backwave amplitude. The amplitude of the control input f, whose role is matching Ψ, approaches one half of Ψ irrespective of ε, according to (7) and (8). We therefore focus on h, whose role is rendering the control wave uni-directional as possible, implying that h is the actual 'hard worker'. We plot the amplitude of h/Ψ (dashed lines), which

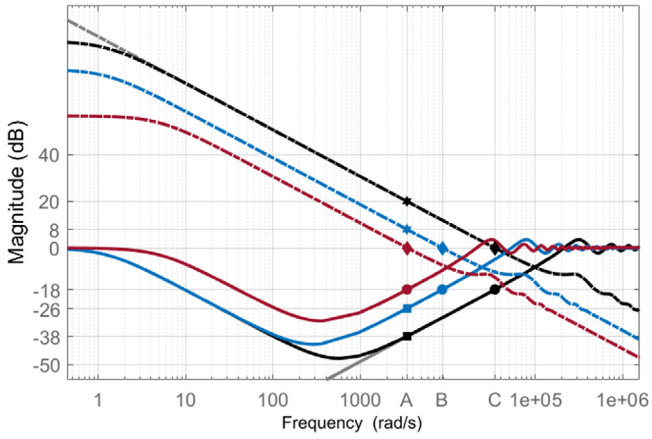

Fig. 4. A frequency response diagram that illustrates the trade-off between the control effort of h and the backwave BW for a given source Ψ. Dashed lines represent the relative control effort $|h|/|\Psi| = |C_h|/|Q|$, given by (3), (8) and (7). Solid lines represent the relative backwave $|BW|/|v_\Psi| = |\overline{Q}|/|Q|$, given by (10) and (2). Red is for $\epsilon = 0.05$, blue is for $\epsilon = 0.02$ and black is for $\epsilon = 0.005$, where $\eta = 500\epsilon$. The case $\eta = 0$ for $\epsilon = 0.005$ is added in grey for comparison. Diamonds represent nominal reduction, which is the reduction in the backwave amplitude that can be achieved for $|h|/|\Psi| = 1$(0 dB). Squares represent backwave reduction at the working frequency $f_0 \approx 540$ Hz (A), which equals -26 dB (20 times) for $\epsilon = 0.02$ (blue) and -38 dB (80 times) for $\epsilon = 0.05$ (red). Stars represent the respective amplitude of h, which equals 8 dB (2.5 times) for $\epsilon = 0.02$ (blue), and 20 dB (10 times) for $\epsilon = 0.05$ (red). (For interpretation of the references to colour in this figure legend, the reader is referred to the web version of this article.)

equals $C_h(s)/Q(s)$ by (3) and (8), and the amplitude of BW/v_Ψ (solid lines), which equals $\overline{Q}(s)/Q(s)$ by (10) and (1), for $\varepsilon = 0.05$ m (red), $\varepsilon = 0.02$ m (blue) and $\varepsilon = 0.005$ m (black), all with $\eta = 500\varepsilon$. For the backwave reductions obtained at the working frequency $f_0 \approx 540$ Hz (Fig. 3), which are 8 (-18 dB), 20 (-26 dB) and 80 (-38 dB) times reduction, the corresponding amplitudes of h (label A in Fig. 4), are given by 1 (0 dB), 2.5 (8 dB) and 5 (14 dB).

It can be observed that although by (6), $\overline{Q}(s) \to 0$ as $\varepsilon,\ \eta \to 0$, $\overline{Q}(s)$ is small only in a certain frequency range. The range becomes wider as ε and η decrease. For $\omega \to 0$ and $\omega \to \infty$ (provided $\eta > 0$), we obtain $\overline{Q}(s) \to 1$. The influence of η, however, becomes indistinguishable from a certain frequency, as demonstrated by the grey lines corresponding to $\varepsilon = 0.005$ m and $\eta = 0$ on top of the black lines. The 0 dB crossing, where the magnitude of h equals that of Ψ, may be regarded as the nominal reduction. It provides an 8 times (-18 dB) reduction of the backwave. It is interesting to note that the nominal reduction is independent of ε. The value of ε only determines at which frequency it occurs. Denoted by diamonds in Fig. 4, the nominal reduction is obtained at frequency $f_0 \approx 540$ Hz (label A) for $\varepsilon = 0.05$ m, $f_0 \approx 1369$ Hz (label B) for $\varepsilon = 0.02$ m and $f_0 \approx 2785$ Hz (label C) for $\varepsilon = 0.005$ m.

4.4. Stability proof of $\frac{1}{Q(s)}$

Since $Q^{-1}(s) = (1 + A(s))^{-1}$ can be regarded as a negative feedback of the stable system $A(s)$, its polar plot must not encircle -1. Here we prove that $|A(j\omega)| < 1$ at all frequencies. We calculate $|A(j\omega)| = \sqrt{2g(\tau_\varepsilon\omega)}$ where $g(\tau_\varepsilon\omega) \doteq (1 - \cos\tau_\varepsilon\omega)/(\tau_\varepsilon\omega)^2 + (\tau_\varepsilon\eta)^2$. The solutions of $g'(\tau_\varepsilon\omega) = 0$ satisfy $1 - \cos\tau_\varepsilon\omega = \sin(\tau_\varepsilon\omega)\left[(\tau_\varepsilon\omega)^2 + (\tau_\varepsilon\eta)^2\right]/2\tau_\varepsilon\omega$ for $\omega > 0$. Substituting back to g yields $g(\tau_\varepsilon\omega) = \sin(\tau_\varepsilon\omega)/2\tau_\varepsilon\omega < 1/2$ for all $\omega > 0$ (where at $\omega = 0$ we have a minimum $g = 0$).

5. Conclusion

The main contribution of this paper is a methodology for creating an active absorber in the interior of a one-dimensional domain, such as a waveguide, for the purpose of wave suppression. Specifically, we considered suppression of wave propagation beyond a prescribed location x_0 (at $x > x_0$) with minimal perturbation backwards (at $x < x_0$). We implemented the absorber with two concentrated actuators, f and h located at x_0, and $-h$ at $x_0 - \varepsilon$. Relating f and h as in (3) we were able to generate a near uni-directional control wave, which was the key element in suppressing the reflectance of the absorber (the control back action wave). We then employed this control wave in two different control algorithms, a feed-forward and a feedback one, denoted by Interior Wave Suppression, whose role was suppressing the transmittance of the absorber. In an acoustic waveguide example we demonstrated how the achievable reduction in the control backwave was traded-off with the amplitude of the h input, which was determined by the distance ε. At a working frequency of 540 Hz, we achieved a reduction of 18 dB, 26 dB and 38 dB in the backwave amplitude with 0 dB, 8 dB and 14 dB amplitudes of the respective control input h.

References

Beranek, L. L., & Mellow, T. J. (2012). *Acoustics: sound fields and transducers*. Academic Press.

Bies, D. A., Hansen, C., & Howard, C. (2017). *Engineering noise control*. CRC Press.

Chakrabortty, A. (2012). Wide-area damping control of power systems using dynamic clustering and TCSC-based redesigns. *IEEE Transactions on Smart Grid*, *3*(3), 1503–1514.

Fu, J.-X., Lian, J., Liu, R.-J., Gan, L., & Li, Z.-Y. (2011). Unidirectional channel-drop filter by one-way gyromagnetic photonic crystal waveguides. *Applied Physics Letters*, *98*(21), 211104.

Graff, K. F. (2012). *Wave motion in elastic solids*. Courier Corporation.

Guo, W., Shao, Z.-C., & Krstic, M. (2017). Adaptive rejection of harmonic disturbance anticollocated with control in 1d wave equation. *Automatica*, *79*, 17–26.

Inman, D. J. (2017). *Vibration with control*. John Wiley & Sons.

Krstic, M., Guo, B.-Z., Balogh, A., & Smyshlyaev, A. (2008). Output-feedback stabilization of an unstable wave equation. *Automatica*, *44*(1), 63–74.

Lesieutre, B. C., Scholtz, E., & Verghese, G. C. (2002). Impedance matching controllers to extinguish electromechanical waves in power networks. In *Control applications, 2002. Proceedings of the 2002 international conference on, Vol. 1* (pp. 25–30). IEEE.

Maeda, K., & Colonius, T. (2017). A source term approach for generation of one-way acoustic waves in the euler and navier–stokes equations. *Wave Motion*, *75*, 36–49.

Rodríguez-Fortuño, F. J., Marino, G., Ginzburg, P., OConnor, D., Martínez, A., Wurtz, G. A., et al. (2013). Near-field interference for the unidirectional excitation of electromagnetic guided modes. *Science*, *340*(6130), 328–330.

Sanchis, L., García-Chocano, V., Llopis-Pontiveros, R., Climente, A., Martínez-Pastor, J., Cervera, F., et al. (2013). Three-dimensional axisymmetric cloak based on the cancellation of acoustic scattering from a sphere. *Physical Review Letters*, *110*(12), 124301.

Sirota, L., & Annaswamy, A. M. (2017). Spatially continuous modeling and control of swing dynamics in electric power grids. *IFAC-PapersOnLine*, *50*(1), 4400–4405.

Sirota, L., & Annaswamy, A. M. (2018). Modeling and control of wave propagation in a ring with applications to power grids. In *Accepted for publication in transactions on automatic control*. IEEE.

Sirota, L., & Halevi, Y. (2010). Free response and absolute vibration suppression of second-order flexible structuresthe traveling wave approach. *Journal of Vibration and Acoustics*, *132*(3), 031008.

Sirota, L., & Halevi, Y. (2014). Wave based vibration control of membranes. In *American control conference (ACC), 2014* (pp. 2729–2734). IEEE.

Sirota, L., & Halevi, Y. (2015a). Fractional order control of flexible structures governed by the damped wave equation. In *American control conference (ACC), 2015* (pp. 565–570). IEEE.

Sirota, L., & Halevi, Y. (2015b). Fractional order control of the two-dimensional wave equation. *Automatica*, *59*, 152–163.

Sumer, E. D., & Bernstein, D. S. (2012). Adaptive decentralized noise and vibration control with conflicting performance objectives. In *Proc. DSCC* (pp. 1–10).

Thorp, J. S., Seyler, C. E., & Phadke, A. G. (1998). Electromechanical wave propagation in large electric power systems. *IEEE Transactions on Circuits and Systems I: Fundamental Theory and Applications*, *45*(6), 614–622.